CHAPTER IV
RESULT AND DISCUSSION

4.1 Preparation and Characterization of Chitosan

4.1.1 Chitosan Production

Shrimp shells consist of three major components which are chitin, calcium carbonate, and protein. Calcium carbonate and protein can be removed by solvent extraction and chitin will be obtained as the remaining substance. Where as chitosan is the name given to the total, partially (majorly) deacetylated form of chitin.

In this research, chitosan was prepared from shells of *Litopeneous vannamei* shrimp by demineralization with HCl, deproteinization with 4% NaOH and deacetylation with 50% NaOH in order to remove the calcium carbonate, protein, and the acetyl group of N-acetyl glucosamine repeating units in shrimp shells, respectively.

Table 4.1 Yield of chitin and chitosan production from shrimp shell

Materials	Yield*(%)
Shrimp shell	100
Product after demineralization	49.65
Product after deproteinization (chitin)	30.63
Product after deacetylation (1st deacetylation)	23.35
Product after deacetylation (2nd deacetylation)	21.98
Product after deacetylation (3rd deacetylation)	18.78
Product after deacetylation (4th deacetylation)	14.66

* dry weight basis

4.1.2 Determination of the Degree of Deacetylation (%DD) of Chitosan

The method used to determine degree of deacetylation of chitosan was based on infrared spectroscopic measurement by Baxter *et al.* (1992). The degree of deacetylation (%DD) was calculated from equation 4.1.

$$DD\ (\%) = 100 - [(A_{1655} / A_{3450}) \times 115] \qquad (4.1)$$

where A_{1655} and A_{3450} are absorbance at 1655 cm^{-1} and 3450 cm^{-1}, respectively.

Chitosan has more extent of amino groups than acetamide groups at C2 position of N-acetyl glucosamine repeating units. The degree of deacetylation of chitosan depends on the nature of chitosan resources and the conditions used during deproteinization. The chitosan used in this study was inevitably subjected to N-deacetylation process under alkaline condition and heating. The result in figure 4.1 shows that the degree of deacetylation (%DD) of chitosan increased with increasing the number of alkali treatment cycles, but the degree of deacetylation (%DD) of chitosan became constant after alkali treatment of chitosan for three times. According to the method of Baxter *et al.* (1992), the degree of deacetylation of chitin calculated from FTIR spectrum in figure 4.2 was 26% and those of chitosan were 85% and 96% for first and second treatment cycles, respectively, and 98% for both third and forth treatment cycles.

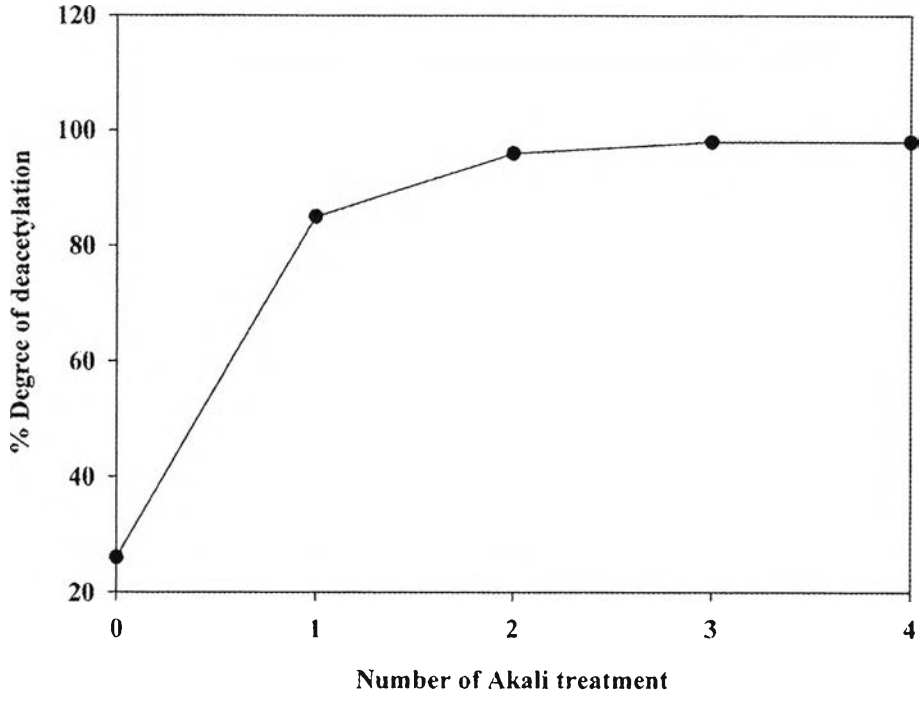

Figure 4.1 Effect of number of alkaline treatment on the degree of deacetylation of chitosan.

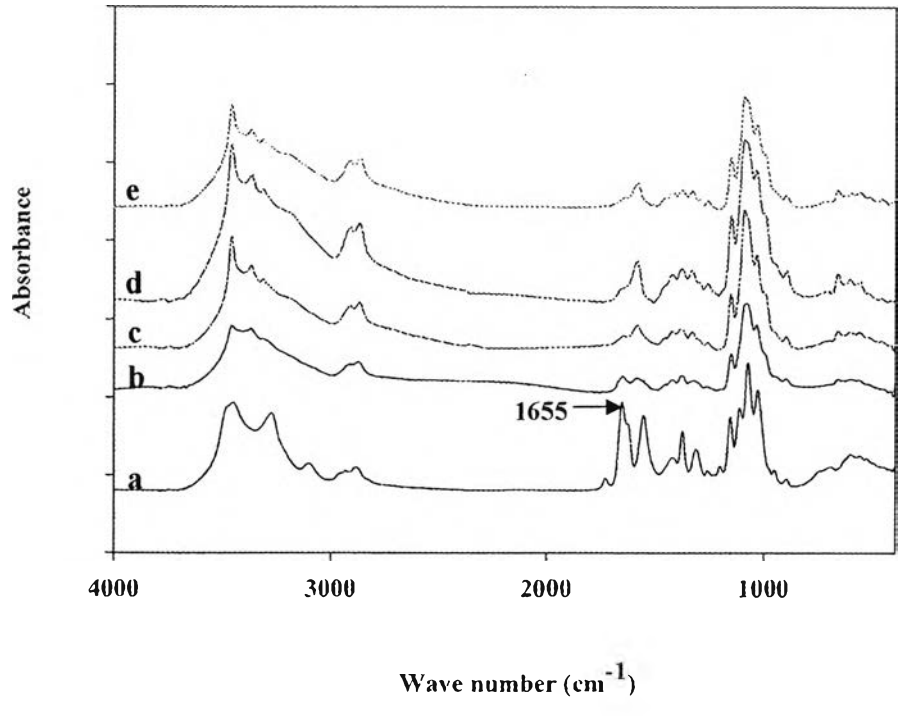

Figure 4.2 FTIR spectra of chitin and chitosan: (a) chitin, (b) 1st deacetylation, (c) 2nd deacetylation, (d) 3rd deacetylation, (e) 4th deacetylation.

4.1.3 Determination of the Molecular Weight of Chitosan

The molecular weight of chitosan was determined based on viscosity measurement by the method of Wang *et al.* (1991). The viscosity-average molecular weight of chitosan was calculated via Mark-Houwing equation (equation 4.2)

$$[\eta] = 6.59 \times 10^{-5} M_v^{0.88} \quad (4.2)$$

where $[\eta]$ = Intrinsic viscosity (dl/g)

M_v = Viscosity-average molecular weight

The intrinsic viscosity was determined from the Y-intercept of the plot between $[\eta_{sp}]/c$ versus chitosan concentration (g/dl) and ln $[\eta_{rel}]/c$ versus chitosan concentration (g/dl).

Table 4.2 Characteristics of chitosan treated samples

Number of alkali treatment	Degree of deacetylation (%DD)	Molecular weight (x 10^5 g/mole)
1	85	7.46
2	96	7.75
3	98	6.27
4	98	4.90

When the number of alkali treatment increased, the degree of deacetylation of chitosan increased whereas molecular weight of chitosan decreased.

4.2 Preparation and Characterization of Modified PET

4.2.1 Contact angle and Wickability Measurement of PET Surface

The results of contact angle and wickability test were shown in table 4.3 and the contact angle images of water-drop were shown in figure 4.3. In the contact angle test, it was observed that the contact angle of de-ionized water on surface of both woven PET and PET film decreased after air-plasma treatment. In the wickability test, it was also observed that, the water absorption time of woven PET decreased after air-plasma treatment. These indicated that their hydrophilicity of woven PET and PET film increased after air-plasma treatment.

Table 4.3 Characteristics of woven PET and PET film before and after air-plasma treatment

Materials	Contact angle (°)	Wickability test (s)
As-received woven PET	96	203
Woven PET after air-plasma treatment	25	10
As-received PET film	101	-
PET film after air-plasma treatment	30	-

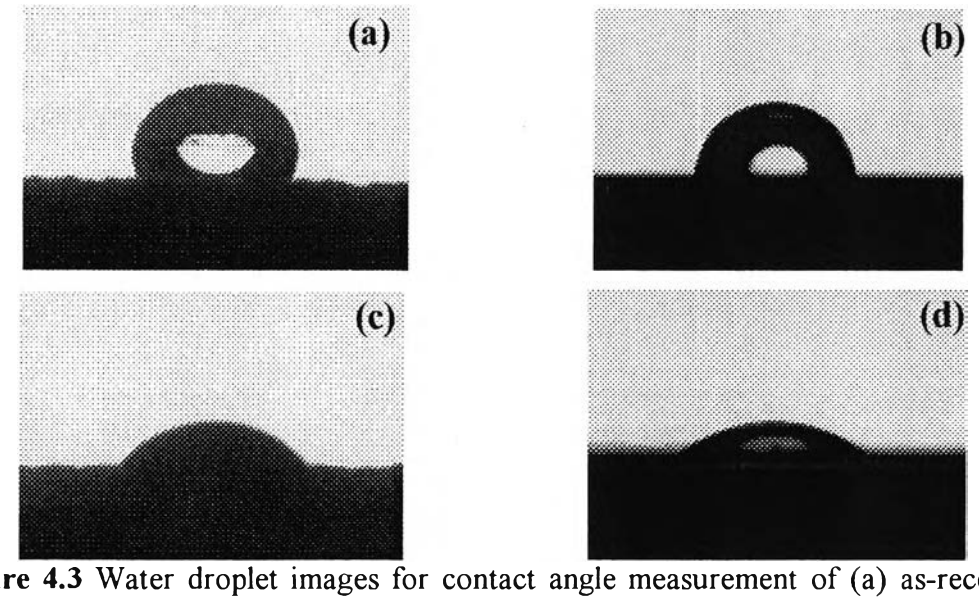

Figure 4.3 Water droplet images for contact angle measurement of (a) as-received woven PET, (b) as-received PET film (c) woven PET after air-plasma treatment, and (d) PET film after air-plasma treatment.

4.2.2 FTIR Spectroscopy

To determine the chemical nature of the surface structure, the infrared spectroscopy with adaptation for the rough surfaces was used. The as-received woven PET fabric and PET film after plasma treatment under air gas were submitted to FTIR analysis. The FTIR spectra of PET film and woven PET fabric are shown in Figures 4.4 and 4.5, respectively. The results show that the most changes between the as-received woven PET fabric and woven PET fabric after plasma treatment under air gas are in the wavenumber range of 400–4000 cm^{-1}. It is also evident that the peak intensity at 732 cm^{-1}, which is attributed to aromatic C–H bond, increased after plasma treatment, but the peak intensity between 2900-2980 cm^{-1}, which is attributed to aliphatic C–H bond, slightly decreased. In addition, the wavenumbers of 1142 and 1730 cm^{-1} can be attributed to C–O and C=O, respectively. After air-plasma treatment, there is a substantial increase in peak intensity at 1260 cm^{-1}, which can be attributed to the O–C=O. Air can generate many active species because when increasing voltage, both nitrogen and oxygen molecules also become fragmented into many active species. Although nitrogen dose not play a significant role in changing the functional groups of woven PET fabric surface, but nitrogen is still an active gas. Active species of nitrogen can possibly collide with oxygen molecule to easily generate more active species. When increasing active species of oxygen, more new functional groups on polymer surface could be obtained, resulting in higher hydrophilicity of woven PET fabric surface.

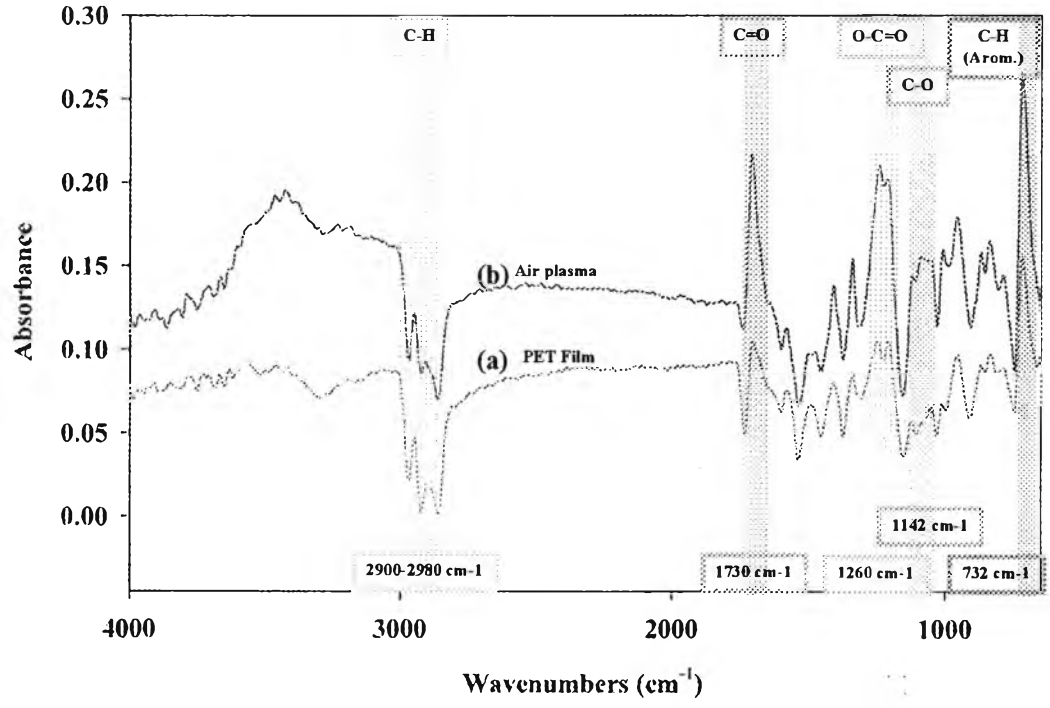

Figure 4.4 FT-IR spectra of PET film with (a) non-plasma treatment (b) air-plasma treatment.

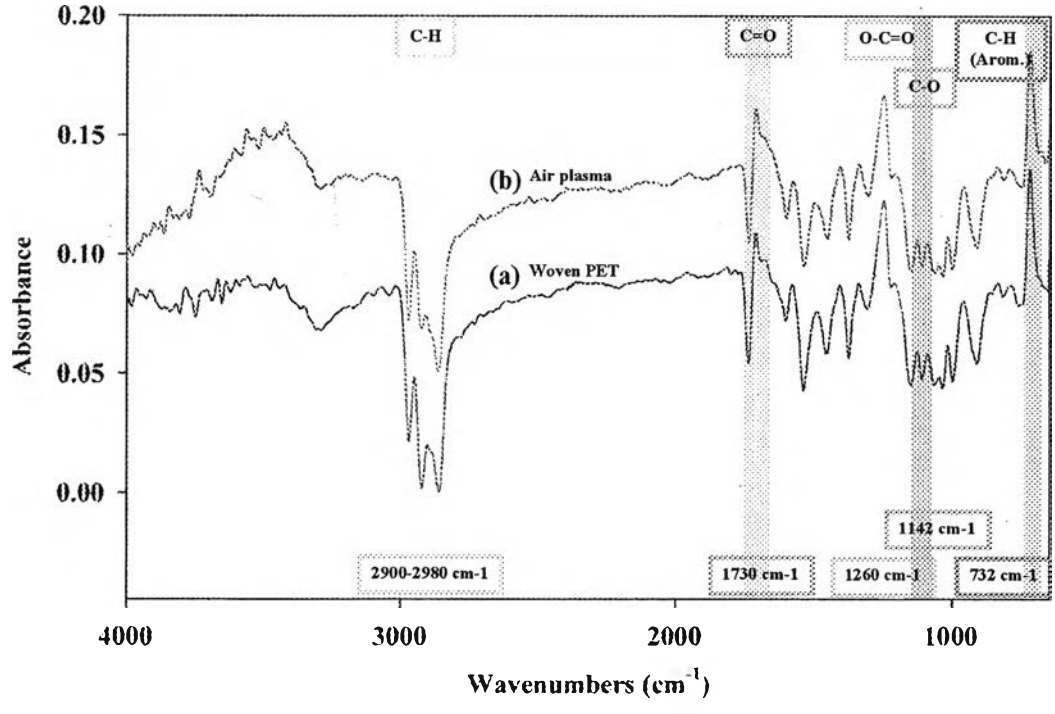

Figure 4.5 FT-IR spectra of woven PET with (a) non-plasma treatment (b) air-plasma treatment.

4.2.3 XPS Analysis

From XPS characterization, a DBD discharge under air at medium pressure can generate a wide range of active species, including atomic oxygen, ozone, nitrogen oxides, neutral and meta-stable molecules, radicals, and ultraviolet radiation. An air plasma increases the surface energy of polymers and textiles by introducing oxygen-containing polar groups onto the polymer surface. Atomic oxygen is believed to be the main reactive species responsible for this oxygen inclusion (Kogelschatz, 2003). Atomic oxygen is formed because of the dissociation of O_2 molecules by electron impact. However, excitation and dissociation of nitrogen molecules also lead to a number of additional reaction paths that can produce additional atomic oxygen (Fang *et al.*, 2001). To investigate what functional groups were formed by plasma treatment, the surface characteristic of the untreated and of plasma-treated samples was examined by XPS.

Figure 4.6 shows the C1s spectra of woven PET fabric surface before and after plasma treatment. The C1s spectra of the woven PET were deconvoluted into 4 components: one at 285.0 eV due to the C–C and C–H groups, one at 286.7 eV due to the CH_2–O– group, one at 289.0 eV due to the O–C=O group, and one at 283.3 eV, which could not be attributed to any specific chemical group. However, it is also possible that the component at 283.3 eV is the result of the broadening of the C1s peak caused by the strong charging of the polyester during the XPS measurements.

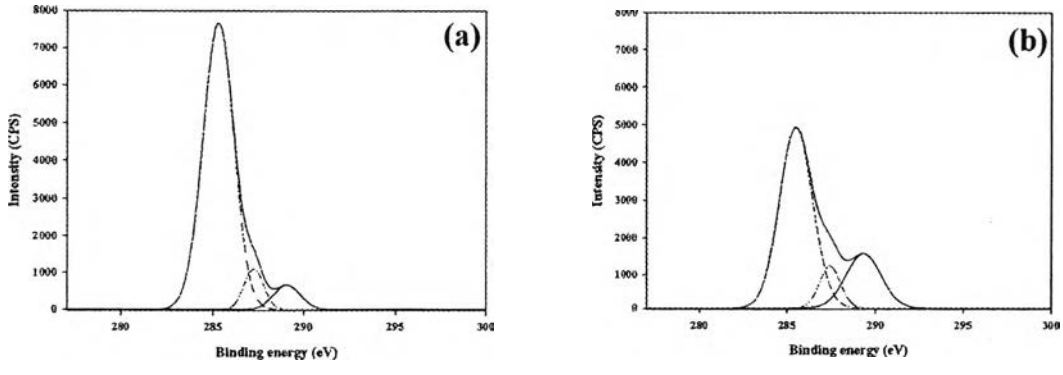

Figure 4.6 Deconvoluted C1s XPS spectra of woven PET (a) before plasma treatment and (b) after plasma treatment (electrode gap distance, 4 mm; treatment time, 10 s; input voltage, 50 V (low side); input frequency, 325 Hz).

Figure 4.6(a) shows the functional group distribution of the as-received woven PET fabric as a function of energy density. The as-received woven PET fabric contains 6.37% C–O group, 7.88% O–C=O group, and 76.84% C–C and C–H groups. The phenyl group on the woven PET fabric surfaces is not presented in Figure 4.6 (a). The concentration of the oxidized carbon components (C–O and O–C=O) increased after plasma treatment (De Geyter *et al.*, 2006).

Figure 4.6(b) also shows that after plasma treatment at medium pressure, the concentration of the C–O and O–C=O groups increased to 16.54 and 11.02%, respectively, while the concentration of the C–C and C–H groups decreased to approximately 68.28%. This means that the air plasma mainly attacks the C–C and C–H groups rather than the ester groups in the polymer chains to form more O–C=O and C–O groups. The introduction of these polar O–C=O and C–O groups is responsible for the higher hydrophilicity of the woven PET fabric after plasma treatment.

4.3 Chitosan Deposition on Plasma-treated PET Surface

4.3.1 Qualitative analysis of chitosan coated on woven PET

To investigate the chitosan coated on woven PET, the qualitative analysis by the colorimetric determination of amino group in chitosan, using amido black 10B is presented. Amido black 10B is an amino acid staining diazo dye used in biochemical research to stain for total amino group of chitosan on the surface of chitosan coated on woven PET. In the figure 4.7 shows the control and modified sample were stained with amido black 10B. There was blue color on the modified sample and colorless on the control, higher amount of amino group on woven PET could be observed when higher chitosan concentration was used in the coating step after plasma treatment. This indicated that air-plasma treatment could improve the adhesion between chitosan and woven PET.

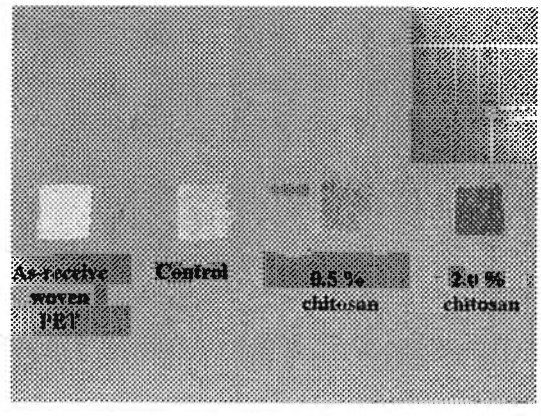

Figure 4.7 Qualitative analysis of chitosan coated on woven PET by using amido black 10B.

4.3.2 Effect of Temperature on Amount of Deposited Chitosan

Figure 4.8 shows the relation between the chitosan concentration and amount of deposited chitosan at room temperature and 50°C coating characterized by Kjeldahl method. The result showed that the temperature had no effect on the chitosan coating.

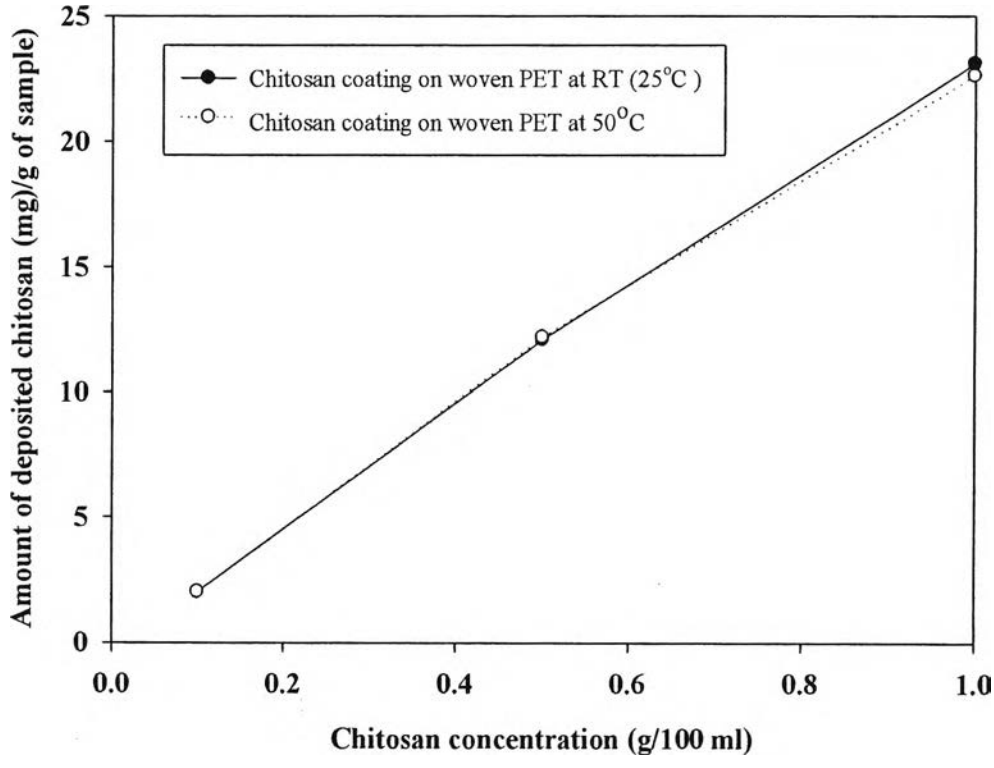

Figure 4.8 Effect of number of temperature on amount of chitosan deposited on woven PET at various chitosan concentrations.

4.3.3 Effect of Number of Washing Cycle on Amount of Deposited Chitosan

Figure 4.9 shows the relation between the number of washing cycle and amount of deposited chitosan characterized by Kjeldahl method. In case of coating with 2% chitosan solution, the result shows that the amount of chitosan deposited on woven PET slightly decreased with increasing the number of washing cycle. After washing woven PET for three times, amount of chitosan on woven PET fabric is constant. On the other hand, in case of coating with 0.5% and 1% chitosan solution, the amount of chitosan deposited on woven PET fabric slightly decreased with increasing the number of washing cycle but amount of chitosan on woven PET fabric was also constant after washing woven PET fabric for three times.

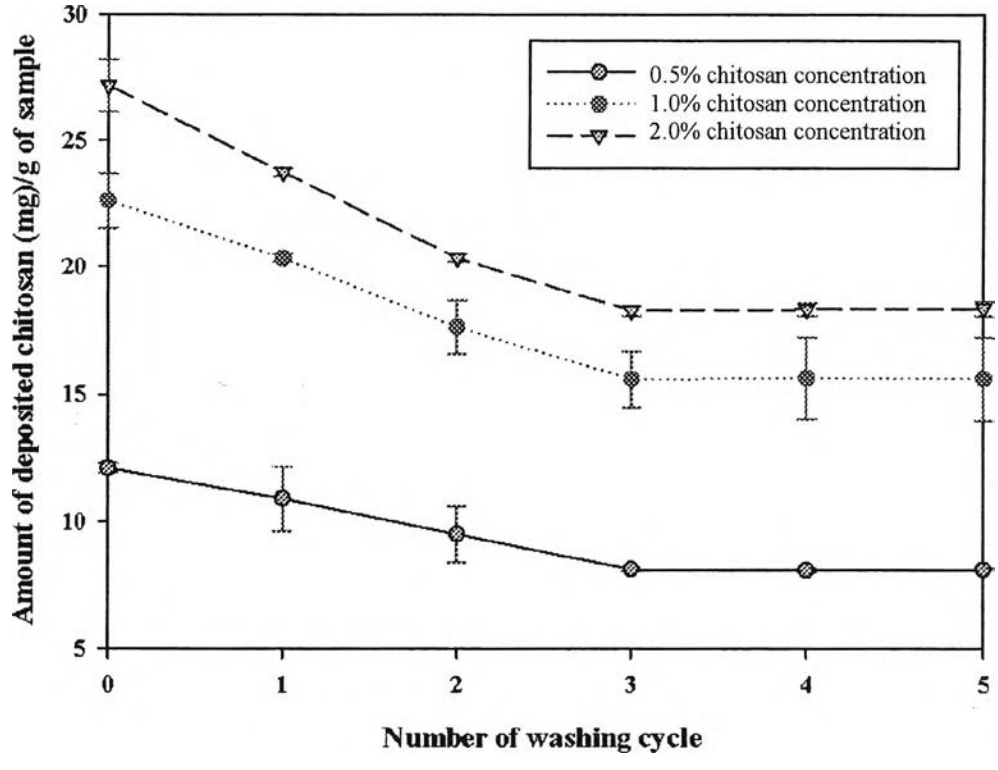

Figure 4.9 Effect of number of washing cycle on amount of chitosan deposited on woven PET at various chitosan concentrations.

4.3.4 Saturated Amount of Chitosan Deposited on Woven PET Fabric

Characterization results from Kjeldahl method were used to find saturated amount of chitosan on woven PET fabric. Figure 4.10 shows the relation between the amount of chitosan deposited on woven PET fabric and chitosan concentration used for chitosan deposition. The results show that the amount of chitosan deposited on woven PET fabric increased with increasing concentration of chitosan from 0.1% to 4% and then remained almost unchanged. Therefore, the saturated amount of chitosan deposited on woven PET was 27.3 mg/g of sample.

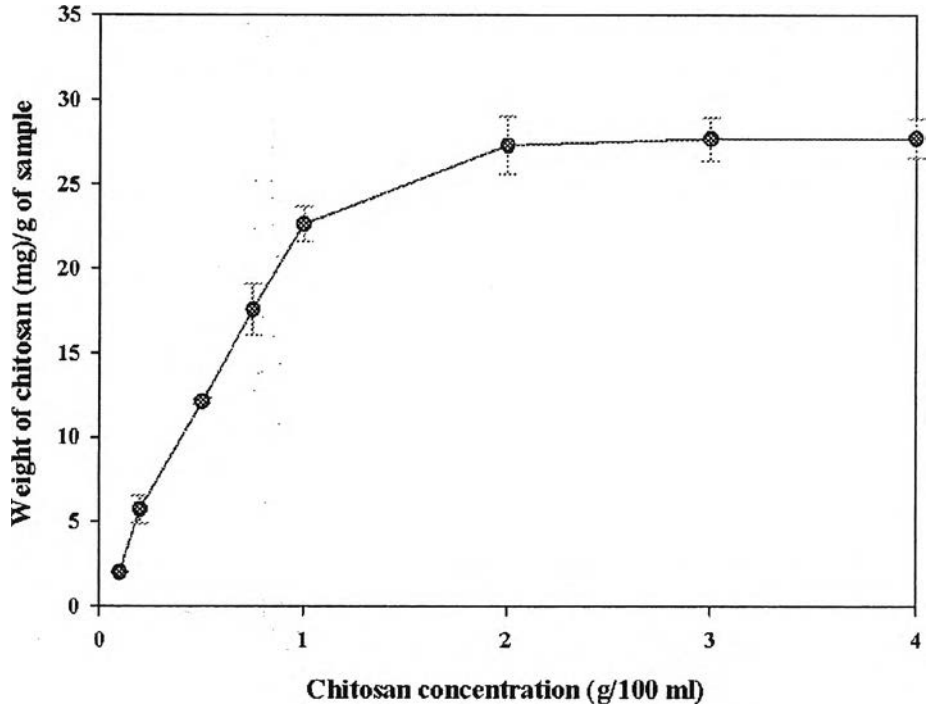

Figure 4.10 Effect of chitosan concentration on amount of chitosan deposited on woven PET.

Results from SEM analysis showed that plasma treatment could enhance the deposition of chitosan on woven PET, as shown in figure 4.11(b) and figure 4.11(c). Figure 4.11(a) shows SEM image of as-received woven PET. Without plasma treatment, there was no change in surface morphology of the woven PET after immersion in 1.0% chitosan solution (Figure 4.11(b)), compared to that of as-received woven PET (Figure 4.11(a)).

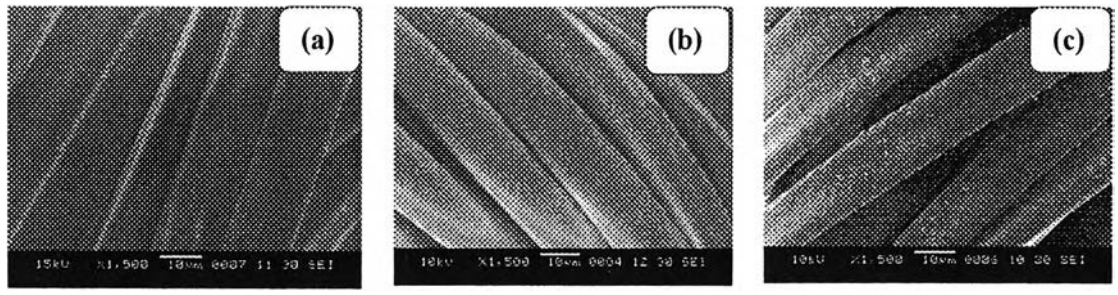

Figure 4.11 SEM images of woven PET fiber (a) without chitosan coating, (b) non-plasma treatment with 1.0% chitosan coating, and (c) plasma treatment with 1.0% chitosan coating.

The chitosan-coated plasma-treated woven PET was also characterized by XPS technique. Figure 4.12 (a) shows the C1*s* spectrum of woven PET after plasma treatment resolved into three individual component peaks: first peak at 285.0 eV, which can be attributed to the carbon in C–C or C–H groups; second peak at 286.7 eV, corresponding to CH_2–O; and third peak at 289.0 eV, due to O–C=O (De Geyter *et al.*, 2006). Figure 4.12 (b) shows the C1*s* spectrum of the 0.5% chitosan-coated woven PET and Figure 4.12 (c) shows the C1*s* spectrum of the 2.0% chitosan-coated woven PET. The ester carbon peak of woven PET at 289.0 eV decreased at 0.5% chitosan-coated woven PET and disappeared completely at 2.0% chitosan-coated woven PET, suggesting that the surface of woven PET was fully covered with chitosan coating (Zhang *et al.*, 2003). Accordingly, it would appear that the ester groups of treated woven PET reacted with the primary amine groups in chitosan, resulting in the generation of amide bonds (-CONH-).

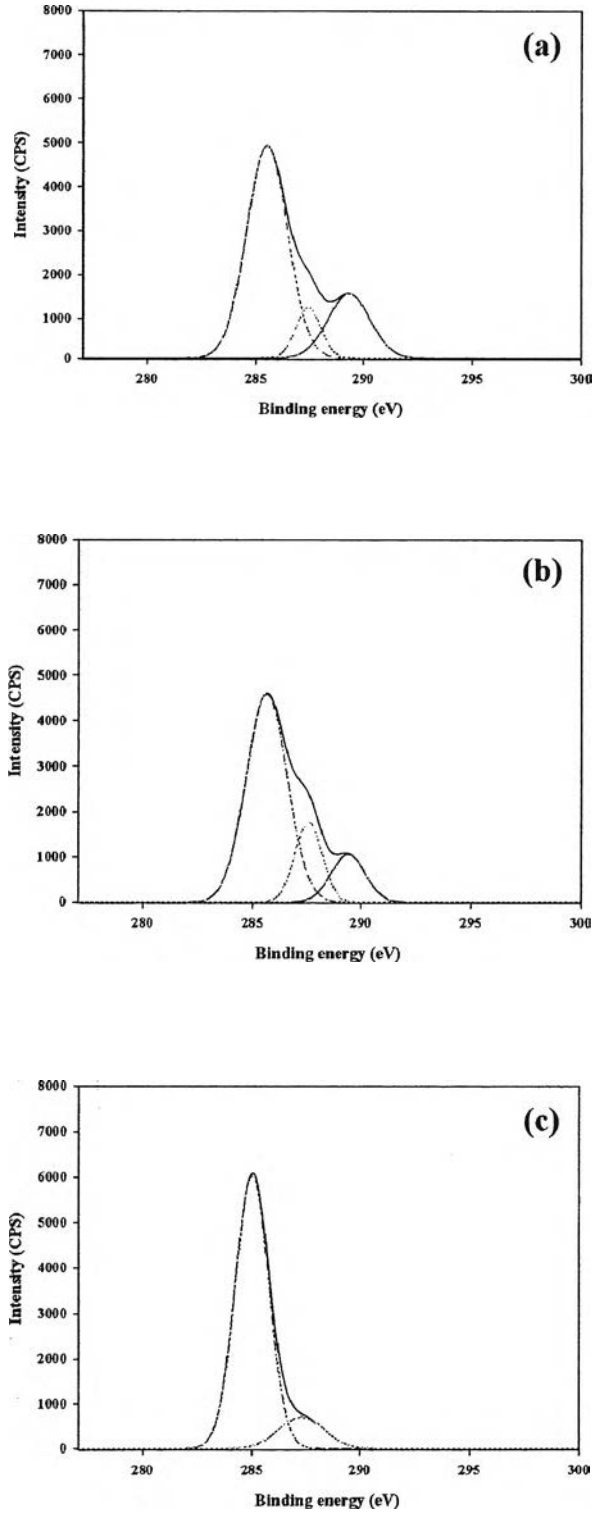

Figure 4.12 Deconvolted C1s XPS spectra of woven PET (a) after plasma treatment, (b) 0.5% chitosan coated plasma-treated woven PET, and (c) 2.0% chitosan coated plasma-treated woven PET.

Figure 4.13 shows the N1s spectra of the chitosan coating located at 400 eV binding energy (Huh *et al.*, 2001), is attributed to the amino nitrogen ($-NH_2$) in chitosan. Upon increasing the chitosan concentration, the peak intensity was also increased.

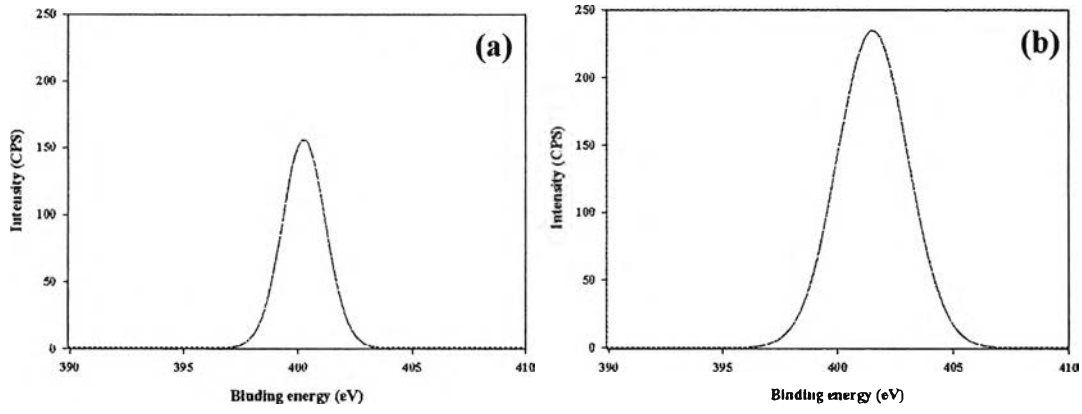

Figure 4.13 N1s XPS spectra of chitosan-coated woven PET (a) woven PET coated with 0.5% chitosan concentration, and (b) woven PET coated with 2.0% chitosan concentration.

4.4 Antimicrobial Activity Testing

4.4.1 Effect of Concentration of Chitosan Solution and Degree of Deacetylation (%DD) on Clear Zone Distance

For this section, the concentration of chitosan solution and degree of deacetylation (%DD) were varied to find the condition that has a clear zone (anti-microbial testing).

This study was divided into two paths. In the first one, the woven PET was submerged into chitosan solution with 85% of degree of deacetylation. For the second path, the woven PET was submerged into chitosan solution with 98% of degree of deacetylation.

In the case where the woven PET was submerged into chitosan solution with 85% of degree of deacetylation, there was no clear zone with every concentration of chitosan solution. On the other hand, the woven PET was submerged into chitosan solution with 98% of degree of deacetylation had a clear zone at the concentration of chitosan solution starting at 0.5% (in the case of *S. aureus*) and 0.75% (in the case of *E. coli*). Antibacterial efficiency against *E.coli* was lower than that against *S.aureus*, probably because of the difference in cell walls between gram-positive and gram-negative bacteria. A decisive structural difference between gram-negative and gram-positive bacteria can be recognized from the molecular structure of the outer cell membrane. In gram-negative bacteria, phospholipids, lipopolysaccharides and proteins exist in the outer membrane. Therefore, electric interaction hardly influences the inner membrane. In contrast, in gram-positive bacteria, the electric charge of chitosan acts directly on the inner membrane of the cell. The electric interaction between chitosan and the cell membrane is one factor inducing bacterial growth inhibition, cell destruction, and activity depression (Takahashia *et al.*, 2007).

The effects of concentration of chitosan solution and degree of deacetylation (%DD) on the anti-microbial activity of woven PET are shown in Figure 4.14. The anti-microbial activity of woven PET (clear zone range) increased with increasing concentration of chitosan solution in the range concentration of 0.1% to 1.0%.

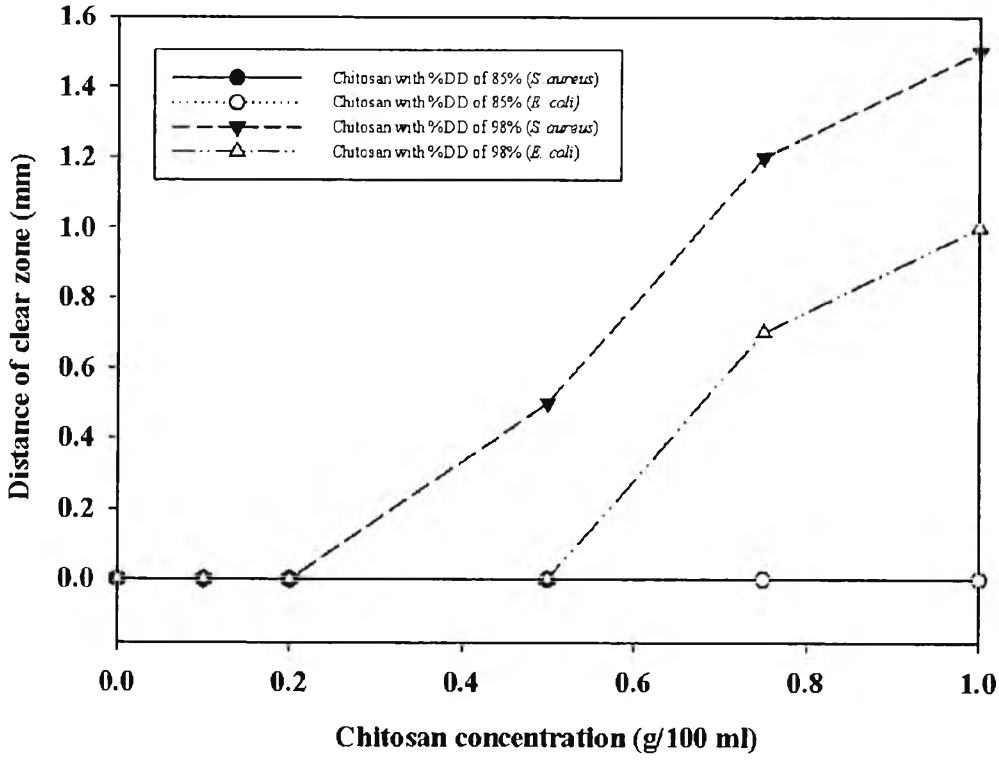

Figure 4.14 Effect of concentration of chitosan solution and degree of deacetylation (%DD) on clear zone distance.

4.4.2 The Disk Diffusion Method

The antibacterial activity of chitosan-coated plasma-treated woven PET fabric for *E. coli* and *S. aureus* was measured by the disk diffusion method. It was found that woven PET with deposited chitosan exhibited an inhibition zone. Figure 4.15 shows that woven PET fabric, which was submerged into chitosan solution, exhibited a clear zone at the 0.5% chitosan concentration in the case of *S. aureus* and 0.75% in the case of *E. coli*. Antibacterial efficiency against *E. coli* was lower than that against *S. aureus*, probably because of the difference in cell wall characteristic between gram-positive and gram-negative bacteria.

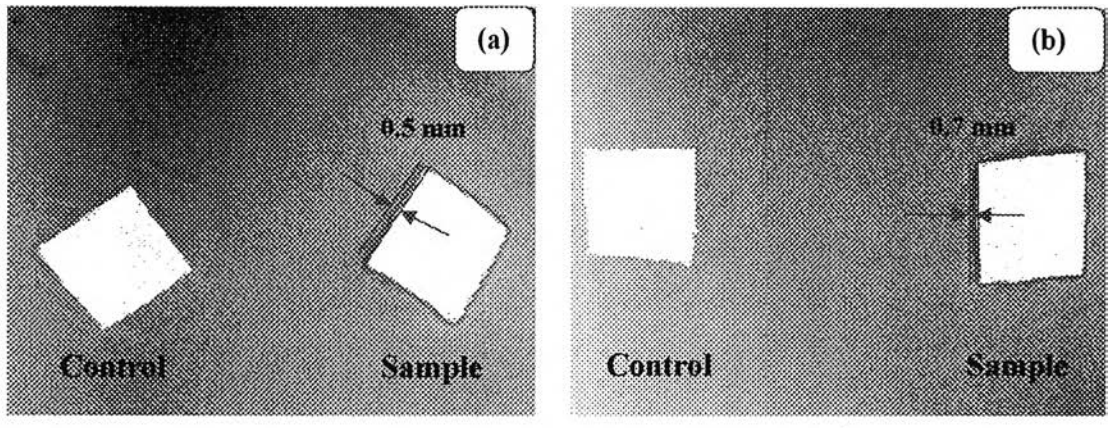

Figure 4.15 The antibacterial activity of plasma-treated woven PET against (a) *S. aureus* (woven PET coated with 0.5% chitosan concentration) and (b) *E. coli* (woven PET coated with 0.75% chitosan concentration)

4.4.3 The Colony Forming Count Method

The chitosan-coated plasma-treated woven PET was also tested for antimicrobial activity against *E. coli* and *S. aureus* by using the colony forming count method. No bacterial growth was observed from the sterility control. The viable counts recovered from the chitosan-coated plasma-treated woven PET fabric before and after incubation are shown in Table 4.4. After 48 h of incubation, there was a 99.99% and 99.90% reduction in viable *S. aureus* and *E. coli*, respectively on the chitosan-coated plasma-treated woven PET. For as-received woven PET fabric, there was no reduction in viable counts; on the contrary, there were 43.91 and 39.26% increases in the viable cell counts of *S. aureus* and *E. coli*, respectively.

Table 4.4 Colony forming unit counts (cfu/ml) at 0-h and 24-h contact time intervals with chitosan coating after plasma treatment of woven PET against *E. coli* and *S. aureus*

Contact time	*S. aureus*			*E. coli*		
	Chitosan coated-woven PET (cfu/ml)	Woven PET (cfu/ml)	Blank (cfu/ml)	Chitosan coated-woven PET (cfu/ml)	Woven PET (cfu/ml)	Blank (cfu/ml)
0 h	3.73×10^{8}	3.62×10^{8}	3.94×10^{8}	3.04×10^{8}	3.07×10^{8}	3.09×10^{8}
24 h	3.40×10^{4}	5.17×10^{8}	6.07×10^{8}	2.89×10^{5}	4.28×10^{8}	4.58×10^{8}
% of reduction / increase	99.99% reduction	43.91% increase	53.98% increase	99.9% reduction	39.26% increase	47.84% increase